JOC The Journal of Organic Chemistry

Article

pubs.acs.org/joc

Tuning the Electronic Properties of 2-Cyano-3-phenylacrylamide Derivatives

Ramachandran Gunasekar,[†,‡] Pichandi Thamaraiselvi,[§] Ravindranath S. Rathore,[∥] Kulathu Iyer Sathiyanarayanan,[*,†] and Shanmugam Easwaramoorthi[*,§]

[†]Chemistry Division, School of Advanced Sciences, VIT University, Vellore 632014, India

[‡]Research Center for Materials Science and the Department of Chemistry, Nagoya University, Chikusa, Nagoya 464-8602, Japan

[§]Chemical Laboratory, CSIR-Central Leather Research Institute, Adyar, Chennai 600020, India

[∥]Department of Biotechnology, School of Life Sciences, University of Hyderabad, Hyderabad 500046, India

Supporting Information

ABSTRACT: We are the first to report the synthesis of a new class of 2-cyanoarylacrylamide (2-CAA) derivatives and observe that the synthesized 2-CAA shows fluorescence properties due to the formation of a dimeric interaction of hydrogen bonds between carbonyl oxygens and amide hydrogens (C═O···H−N−C═O···H−N···); i.e., dimers are linked through dimeric N−H···O hydrogen bonds. The single-crystal X-ray structure shows molecules to be hydrogen-bonded dimers, which further form a parallel stacking arrangement, mediated by significant $\pi-\pi$ interactions. The ^{1}H NMR and fluorescence spectral studies indicate the coexistence of amide and iminol tautomers in solution, which can be influenced by the nature of the solvent. Further, the excitation-wavelength-dependent fluorescence spectrum and the biexponential fluorescence decay profiles suggest the presence of more than one emitting species; i.e., amide and iminol tautomers coexists in solution. We have also shown that the equilibrium between the two tautomers can be tuned by the judicious choice of electron-donating or -withdrawing substituents.

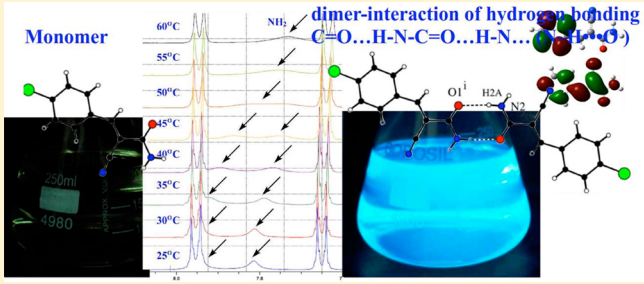

INTRODUCTION

Studies on molecules having an intense color and stronger fluorescence are always of great interest due to their applications as dyes; fluorescent probes; sensors for anions, cations, and neutral molecules; light emitters in organic light-emitting diodes; sensitizers in solar cells; etc. Indeed, these are one of the molecular level spectroscopic tools employed for the detection and monitoring of specific properties or functions of the medium they are incorporated in. These kinds of applications are possible due to the sensitivity of fluorescence properties with respect to temperature, pH, viscosity, polarity, and rigidity of the surrounding environment.[1−5] The preferred configuration for molecules with environment-sensitive fluorescent properties is the presence of electron-donating and -withdrawing substituents connected covalently through intervening π-conjugation. This feature offers a unique choice of designing the new fluorophores having desired properties with the judicious choice of available electron-donating and -withdrawing moieties in different permutations and combinations. In this regard, molecules based on the 3-phenylacrylonitrile skeleton were known to show moderate to excellent fluorescent properties depending upon the substituents. For example, the diphenylacrylonitrile (cyanostilbenes) derivatives gained much attention owing to their unique, tunable, highly responsive luminescent characteristics.[6−9] Particularly, aggregation-induced emission enhancement (AIEE) of cyanostilbene derivatives in their nano- or microaggregated state and crystalline states has been promising in terms of their applications in light-emitting devices. The emission enhancement is caused by the aggregation-induced planarization, which prevents the nonradiative decay pathways due to isomerization. Thus, considering the importance of phenyl acrylonitrile derivatives,[10] we have synthesized new molecules based on 2-cyano-3-arylacrylamide (2-CAA) having different electron-donating and -withdrawing substituents as fluorescent probes. The combination of electron-donating aryl groups and the electron-withdrawing 2-cyanoacrylamide moieties makes these molecules excellent chromophores. For example, 2-cyano-3-[4-aminophenyl]-2-propenamide derivatives show solvatochromism in fluorescence due to intramolecular charge transfer interactions between the donor (diarylamine) and acceptor (2-cyanoacrylamide) moieties; however, systematic studies have not been reported yet.[11] Bosch et al. have demonstrated that naphthalene-based 2-CAA can be used to probe the photopolymerization reaction by virtue of changes in fluorescence intensity in real time.[12−14] Further, the (*E*)-2-cyano-3-(1*H*-indol-3-yl)acrylamide scaffold

Received: September 28, 2015
Published: November 12, 2015

DOI: 10.1021/acs.joc.5b02226
J. Org. Chem. 2015, 80, 12351−12358

has also been used as a tricyclic CRTh2 receptor.[15] In addition, Zhang and co-workers have shown that the *p*-dimethylamino-substituted 2-CAA derivative exhibits piezofluorochromic properties wherein the yellow-green compound was converted to orange-red simply by grinding with a pestle and mortar, and the reversible conversion was possible through heating the sample at 80 °C.[16] It should also be noted that the strong, complementary intermolecular hydrogen bonding between the amine proton and carbonyl group of amide moiety are susceptible to show reversible amide ↔ iminol tautomerism. Hence, to evaluate the electronic properties and explore the feasibility of amide ↔ iminol tautomerism and their consequences on the photophysical properties, we have synthesized a series of 2-CAA derivatives substituted with electron-donating and -withdrawing groups. We are the first to observe that the synthesized 2-CAA shows fluorescence properties due to the formation of a hydrogen-bonded dimeric interaction between carbonyl oxygens and amide hydrogens (C═O···H−N−C═O···H−N···); i.e., dimers are linked through dimeric N−H···O hydrogen bonds. We found that some of the 2-CAA derivatives exhibit excitation-wavelength-dependent fluorescence that could possibly originate from the coexistence of both tautomers in solution. The time-resolved fluorescence study also reveals the presence of two different light-emitting species in solution.

RESULTS AND DISCUSSION

The intensely green fluorescent target compound (*E*)-2-cyano-3-phenylacrylamide (**3a**) shown in Chart 1 has been synthesized, in quantitative yields, by using Knoevenagel condensation between the cyanoacetamide and benzaldehyde in the presence of a catalyst.

Chart 1. Phenylacrylamide Derivatives

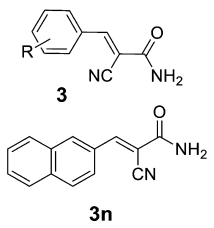

	R		R
3a	H	**3h**	*m*-F
3b	*p*-OCH_3	**3i**	*o*-F
3c	*o*-OCH_3	**3j**	*p*-Cl
3d	*p*-CH_3	**3k**	*o*-Cl
3e	m-CH_3	**3l**	*p*-Br
3f	*o*-CH_3	**3m**	*p*-CN
3g	*p*-F		

Several reaction conditions were adopted to optimize the catalyst, catalyst concentration, and solvent, and the details are summarized in Table S1 of the Supporting Information (SI). It can be understood from Table S1 that the reaction did not preceded without the catalyst, and 1 mol % of sodium hydroxide was found to give relatively higher yields. Further, better yields were obtained when a protic solvent, such as ethanol, methanol, or isopropyl alcohol, was used. Importantly, the product obtained using solvents like acetonitrile, dichloromethane, benzene, and hexane was a nonfluorescent compound, whereas the one obtained by using ethanol, methanol, and isopropyl alcohol was found to be fluorescent in nature. Nevertheless, ^{1}H and ^{13}C NMR spectra confirm the formation of (*E*)-2-cyano-3-phenylacrylamide irrespective of the solvent used for the synthesis. It is really intriguing that the solvent used for synthesis has a major role in determining the fluorescent properties of the resultant product, even when the structures are the same. To our surprise, an identical compound reported in the literature was known to be a nonfluorescent molecule.[17] It is also to be noted that the melting point of **3a** was found to be slightly higher, ca. 10 °C, than the reported one.[17] Though this behavior is not clearly understood, we believe that the presence of intermolecular hydrogen bonding in **3a** might have influenced the fluorescence properties. We have also synthesized the series of compounds possessing 2-cyano-3-arylacrylamide (2-CAA) substituted with electron-withdrawing or -donating groups, as shown in the Chart 1.

The single-crystal X-ray structure of one of the derivatives, i.e., **3j**, for which data collection from a quality crystal could be obtained, was determined. The structure of **3j** shown in Figure 1 reveals planar molecules forming an (amide)N−H···O-(amide)-bonded $R^2_2(8)$ molecular dimer, for which the intermolecular N2−H2···O1^{i} [symmetry code: (i) 2 − *x*, 2 − *y*, −*z*] hydrogen bond, the H···O, N···O distances, and angle N−H···O are respectively measured to be 2.03 Å, 2.887(3)Å, and 174°. Crystal packing is further characterized by molecular dimers associated into a parallel-stacking arrangement, with a Cg1···Cg1^{ii} [symmetry code: (ii) *x*, 1 + *y*, *z*] centroid-to-centroid distance of 3.8750(13) Å, parallel distance of 3.4634(9)Å, and a slippage of 1.739 Å, where Cg1 denotes the centroid of the (C1−C6) aryl ring.

The presence of intermolecular H-bonded amide dimers and possible π-electron delocalization in amide is expected to facilitate the amide ↔ iminol tautomerism. Indeed, ^{1}H NMR studies, as shown in Figure 2, reveal the two broad singlets for the amide protons at 7.83 and 7.96 ppm in DMSO-d_6, instead of one broad singlet generally observed for the amide proton at 7.96 ppm,[12] and also the chemical shift values of these protons further shifted to 5.90 and 6.33 ppm in $CDCl_3$.

We have recorded NMR for **3j** in the range from 25 to 60 °C and found that the peak at 7.85 ppm remains a singlet at 50−60 °C, whereas at 25−45 °C the peak at 7.85 ppm shifts toward an upfield region and splits from a broad singlet in to a doublet at

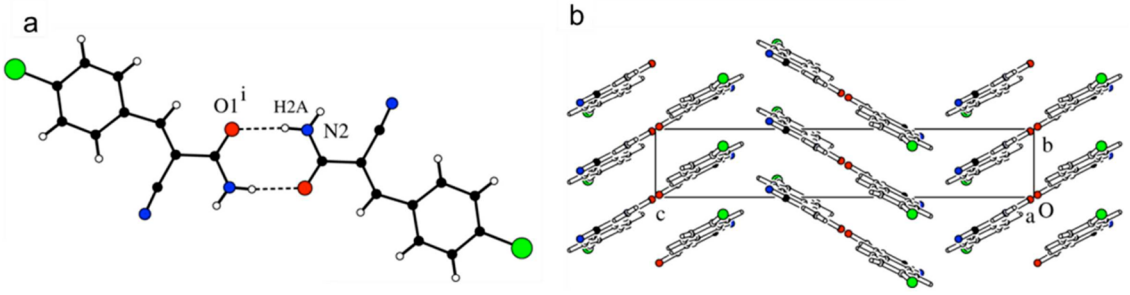

Figure 1. (a) Dimeric association of **3j** linked through (amide)N−H···O(amide) hydrogen bonds. (b) Molecular stacking, shown in a crystal-packing view projected onto the *bc*-axis, highlighting molecular aggregation via $\pi\cdots\pi$ interactions also in addition to dimeric association.

DOI: 10.1021/acs.joc.5b02226
J. Org. Chem. 2015, 80, 12351−12358

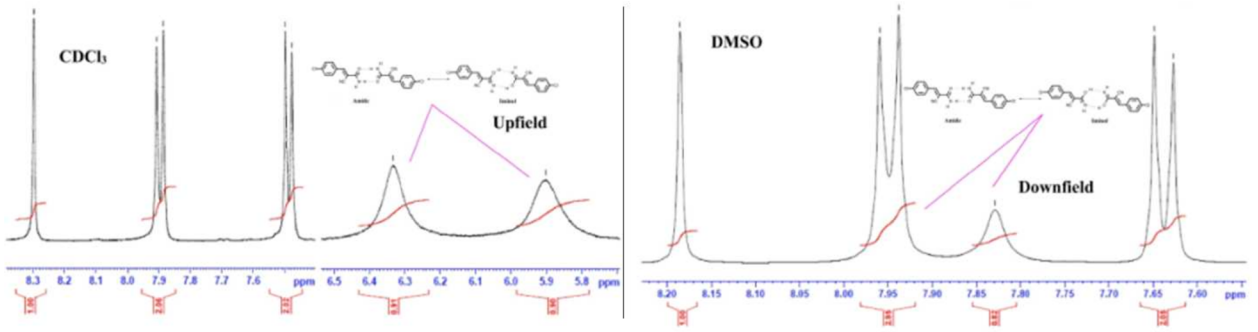

Figure 2. Chemical shift of 2-cyano-3-(4-chlorophenyl)acrylamide (**3j**) in DMSO-d_6 and $CDCl_3$.

7.9 ppm (Figure 3). This clearly supports the evidence for the formation of intermolecular hydrogen bonding between the

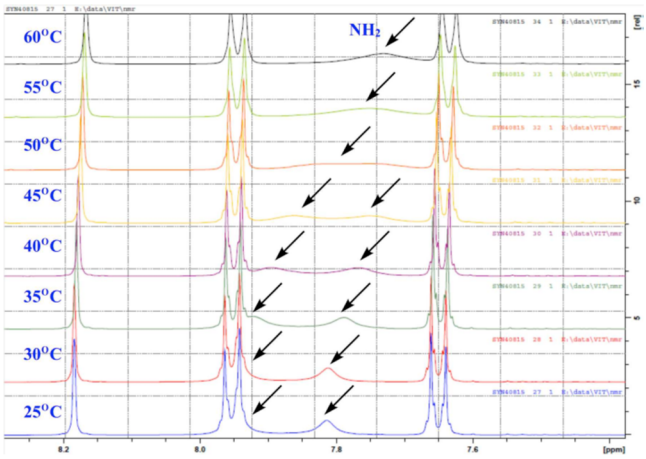

Figure 3. ^{1}H NMR spectrum of 2-cyano-3-(4-chlorophenyl)-acrylamide (**3j**) in DMSO at high temperature from 7 to 8 ppm.

amide hydrogen and carbonyl oxygen. In our previous report,[18] we described the synthesis of triazatricyclo[6.2.2.0^{1,6}]dodecane-9,12-dione (TATCD) derivatives. In the previous report, the synthesized TATCD derivatives possess a fluorescence property due to the formation of the 2-CAA intermediate; thus, the fluorescence property of this 2-CAA molecule is retained in order for the TATCD derivatives to exhibit fluorescence. The presence of two different peaks for the protons attached to the amino nitrogen can be asscribed to the coexistence of amide ↔ iminol tautomers in solution. The electronic properties of 2-CAA derivatives were studied by UV−visible absorption as well as steady-state and time-resolved fluorescence spectroscopic techniques. UV−visible absorption spectra of the all the samples were recorded in chloroform, and the data are summarized in Table 1.

The representative absorption and fluorescence spectra of compounds (*E*)-2-cyano-3-phenylacrylamide (**3a**) and (*E*)-2-cyano-3-(naphthalen-2-yl)acrylamide (**3n**) dissolved in chloroform solvent are depicted in Figure 4. Both the compounds

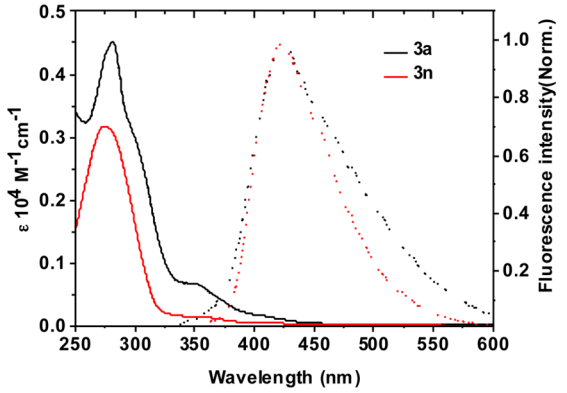

Figure 4. UV−visible absorption (solid line) and fluorescence (dotted line) spectra of **3a** (black) and **3n** (red) in chloroform solvent. The samples were excited at 357 nm.

Table 1. Photophysical Properties of Phenylacrylamide Derivatives in Chloroform Solvent

entry	substituent	λ_{abs}, nm ($\varepsilon 10^4$ M^{-1} cm^{-1})	λ_{fl}, nm	Stokes shift, cm^{-1}	τ_1, ns	relative amplitude	τ_2, ns	relative amplitude	τ_{avg}, ns
3a	H	280 (0.459), 357 (0.069)	424	4482	1.16	60.4	4.72	39.6	2.63
3b	*p*-OCH_3	270 (0.689), 391 (0.065)	437, 460	3836	2.48	100	–	–	–
3c	*o*-OCH_3	270 (0.496), 392 (0.116)	437, 460	3771	1.97	100	–	-	-
3d	*p*-CH_3	270 (2.32), 390 (0.24)	430, 456	3711	2.55	100	–	–	–
3e	*m*-CH_3	269 (0.643), 400 (0.097)	433, 458	3165	2.53	100	–	–	–
3f	*o*-CH_3	274 (0.134), 394 (0.008)	435, 455	3210	1.74	100	–	–	–
3g	*p*-F	268 (0.424), 350 (0.17)	415	4475	0.38	47.67	1.42	52.33	0.92
3h	*m*-F	360 (0.48)	414, 444	4950	0.62	29.71	2.16	70.23	1.70
3i	*o*-F	280 (1.86), 357 (0.64)	442	4999	1.58	51.93	3.72	48.07	2.10
3j	*p*-Cl	351 (1.19)	434, 461	6798	1.03	57.90	4.46	42.10	2.47
3k	*o*-Cl	282 (1.08), 352 (0.36)	421	4656	1.04	23.41	5.59	76.56	4.52
3l	*p*-Br	278 (0.657), 356 (0.53)	424, 463	6491	1.05	27.25	3.61	72.75	2.85
3m	*p*-CN	275 (0.585), 350 (0.167)	423	4931	1.08	22.24	3.99	77.76	3.34
3n	–	276 (0.317), 357 (0.023)	424	4482	1.60	44.09	3.86	55.91	2.86

DOI: 10.1021/acs.joc.5b02226
J. Org. Chem. 2015, 80, 12351−12358

show the lowest energy absorption band at 357 nm and the highest energy peak around 280 nm. The extended π electron conjugation for **3n** compared to **3a** does not alter the $S_0 \rightarrow S_1$ transtion energy, but the molar extinction coefficient values and relative intensities are found to be characteristic of the aryl groups. The lowest energy peak has been attributed to the transition from singlet ground (S_0) to the first excited state (S_1), $S_0 \rightarrow S_1$.

The fluorescence spectra of **3a** and **3n** were observed at 424 nm having a mirror image relationship with their respective lowest energy absorption band. The Stokes shift value was calculated to be ~4480 cm^{-1} for both **3a** and **3n**. The higher Stokes shift value suggests that significant structural changes occur during the transition from ground to an excited state. Further, the presence of the cyanoacrylamide moiety, a strong acceptor group, connected to the aromatic ring through intervening π-conjugation probably induces the intramolecular charge transfer (ICT) character, which would also be responsible for the observed larger Stokes shift values. To get further insight on the ICT interactions, we have calculated frontier molecular orbitals using the Gaussian 03 program.[19]

The crystal structure of **3j** was used as an input file for the TD-DFT calculations. The highest occupied molecular orbitals (HOMO) and lowest unoccupied molecular orbital (LUMO) were calculated at the B3LYP/6-31G level using the optimized geometries at the same level of theory. As can be seen from the Figure S1 (SI), most of the electron density was found to be localized on the aryl ring in the HOMO, whereas in the LUMO it was localized on the cyanoacrylamide moiety. The electron density redistribution during the transition from HOMO to LUMO suggests the existence of intramolecular charge transfer interactions, which in fact can be influenced by the nature of the substituent and its substitution position (Table S3, SI). In addition, the HOMO and LUMO energy levels were perturbed to a smaller than significant extent by the substituents. Further, a qualitative correlation with respect to electron-withdrawing/donating behavior, a plot of energies of the frontier orbital versus the Hammett parameter ($\sigma+$)[20,21] is shown in Figure 5. While the theoretically calculated HOMO and LUMO energy levels show a linear relationship with the Hammett parameter, no correlation has been observed for the experimental lowest energy absorption maximum (in wavenumbers) versus the Hammett parameter.

Attempts have been made to tune the electronic properties of 2-CAA by introducing the different electron-withdrawing and -donating groups at *o*/*m*/*p*-phenylene positions. The UV−visible absorption spectrum of 2-CAA was found to show significant changes in the spectral pattern with respect to the electron-donating or -withdrawing nature of the substituent.

As can be seen from the UV−visible absorption spectra shown in Figure 6, for the 2-CAA derivatives substituted with an electron-donating group, the lowest energy absorption peak becomes intensified, broadened, and red-shifted by 35−42 nm, characteristic of the substituent. On the other hand, the electron-donating substituents do not show any significant spectral shifts due to substituent position. This feature suggests that the lowest energy absorption band might have originated due to intramolecular charge transfer transition ($S_0 \rightarrow$ CT). Further, careful examination of Table 1 reveals that the molar extinction coefficient for the CT band was sensitive to the substituent position; the presence of bulky group, such as methyl and chlorine, in the ortho position resulted in a decrease of molar extinction coefficient by at least a factor of 3 when

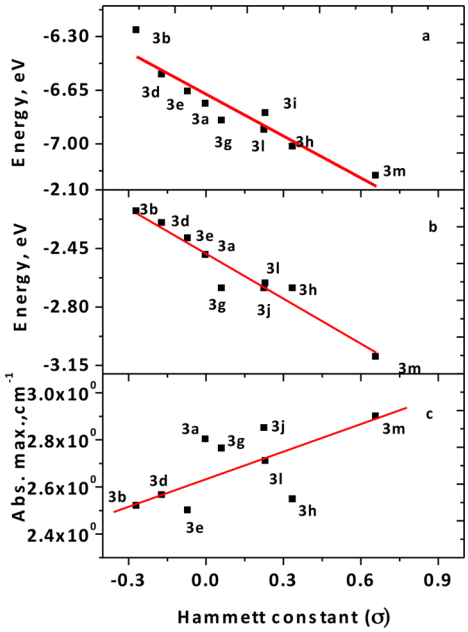

Figure 5. Plots of (a) HOMO energy and (b) LUMO energy calculated using Gaussian 03 and (c) experimental absorption maximum (in wavenumber) versus Hammett constant for phenylacrylamides derivatives.

compared to the respective para-isomers. Similar to the absorption spectra, fluorescence spectra of the substituted 2-CAA show significant changes characteristic of the nature of the substituent as well as to its position in the aromatic ring (Figure S2, SI). Nonetheless, the emission maxima were found to show only marginal changes, ca. 10 nm, with substitution. The electron-donating methyl and methoxy substituents show two emission peaks around 430 and 460 nm, irrespective of the substituent position. In contrast, the electron-withdrawing group fluorine shows substituent-position-dependent fluorescence spectra wherein the meta-isomer show two peaks at 414 and 444 nm, and the ortho- and para-isomers respectively emit at 442 and 415 nm.

Further information about the excited state can be gleaned from the fluorescence lifetime decay profiles shown in Figure 7 obtained using the time-correlated single-photon-counting technique. The decay profiles were fitted with a single or biexponential function, and the data are summarized in Table 1. For **3a**, two lifetimes with the time constants of 1.16 and 4.72 ns with the relative amplitudes of 60.40 and 39.60, respectively, were obtained. The two different lifetimes might have originated from the amide and iminol forms of **3a** at the excited state. Intriguingly, the decay profiles of the compound substituted with electron-donating substituents, such as methyl and methoxy group, was fitted with a single exponential function with the lifetimes ranging from 1.74 to 2.55 ns. Further, the ortho-substituted 2-CAA derivative show comparatively shorter lifetime, ca. ~0.5 ns, than their corresponding para congener, probably due to the steric interaction with the cyanoacrylamide moiety, which would enhance the non-radiative decay. In contrast, the electron-withdrawing substituents shows two fluorescence lifetimes, similar to the parent compound **3a**, but with different time constants and relative amplitude values. The influence of substituent position on fluorescence lifetime can be understood from the longer

DOI: 10.1021/acs.joc.5b02226
J. Org. Chem. 2015, 80, 12351−12358

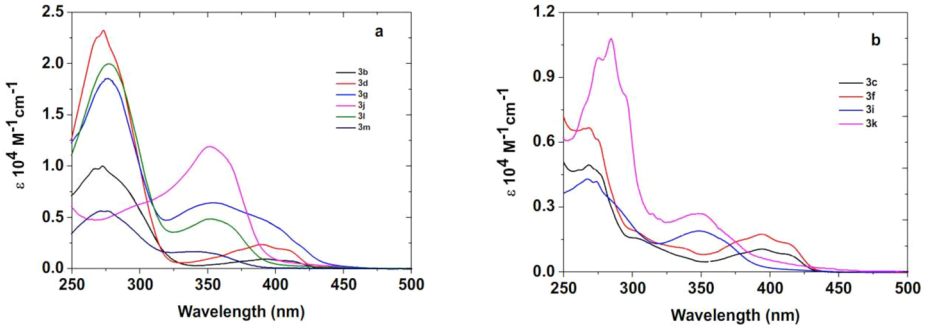

Figure 6. UV−visible absorption spectra of phenylacrylamide derivatives dissolved in chloroform solvent.

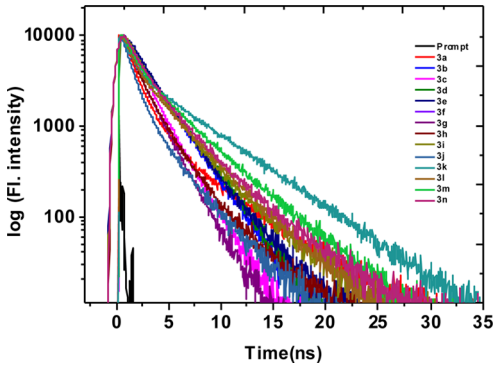

Figure 7. Fluorescence decay profiles of phenylacrylamide derivatives dissolved in chloroform solvent. The decay was monitored at their respective emission maximum wavelength.

lifetime for *o*-fluoro and *o*-chloro substituents by nearly a factor of 2 with respect to the corresponding para-isomers.

The shorter lifetime of the para-isomer is probably due to the fact that the para-isomer favors amide ↔ iminol tautomerism compared to the respective ortho-isomer, which would deactivate the excited state by a nonradiative decay pathway. The possibility of intramolecular charge transfer interactions in 2-CAA derivatives can be understood from the solvent-polarity-dependent photophysical studies using selected compounds. Though a solvent-induced spectral change has been witnessed for **3a**, **3h**, and **3j**, as shown in Figure 8, the observed spectral shift has not been characteristic of that generally observed for the system that shows intramolecular charge transfer interactions. For instance, **3a** in toluene shows two well-resolved emission peaks at 410 and 434 nm along with a shoulder at 460 nm.

Notably, a similar pattern is observed for **3a** in acetonitrile and THF, a broad peak with single maximum, as was observed in chloroform. The molecules with donor−acceptor configuration showing intramolecular charge transfer interactions generally show solvent-polarity-induced red-shifted fluorescence, which has been quantified using a Lippert−Mataga plot. Considering the absence of correlation between the Lippert−Mataga plot and solvent-polarity-induced red-shifted fluorescence, it can be understood that the difference in the spectral pattern would have been due to the coexistence of at least two isomers in solution, and their presence is strongly influenced by the nature of the solvent. This hypothesis is

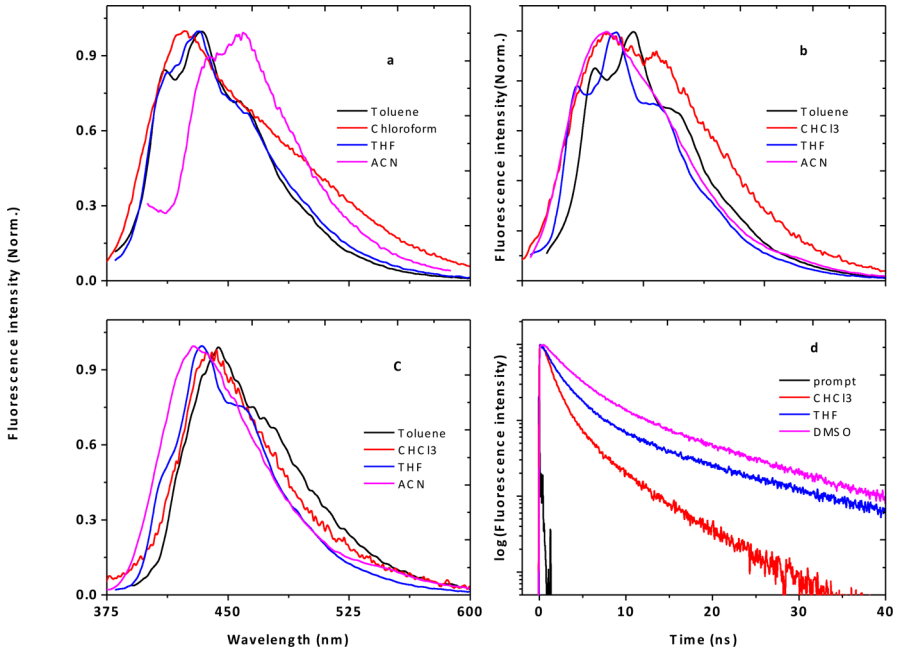

Figure 8. Fluorescence spectra of (a) **3a**, (b) **3h**, and (c) **3j** and fluorescence decay profiles of (d) **3a** dissolved in solvents of different polarity.

DOI: 10.1021/acs.joc.5b02226
J. Org. Chem. 2015, 80, 12351−12358

Scheme 1

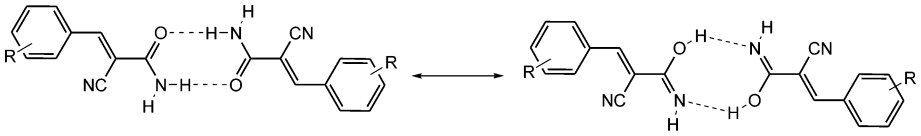

confirmed further by the fluorescence lifetime; the decay profile analysis of **3a** in different solvents given in Figure 8.

The fluorescence lifetime of the long-lived component of **3a** was measured to be 4.72, 9.84, and 11.18 ns, respectively, in chloroform, tetrahydrofuran, and dimethyl sulfoxide. Similarly, the short-lived component also show increased fluorescence lifetime from 1.16 to 2.84 ns while going from chloroform to DMSO along with the decreased relative amplitude. This feature is not clear now; however, we believe that it can be directly related to the hydrogen-bonding dissociation ability of the solvent.

It has been known from the single-crystal X-ray structures shown in Figure 1[22−24] that there exists intermolecular hydrogen-bonding interactions that would favor the isomerism between the acrylamide and iminol form, as shown in Scheme 1. Indeed, the isomerism between the acrylamide and iminol form can be evident from the two broad singlets in the ^{1}H NMR spectra, corresponding to the two protons in a different environment (Figures 2 and 3). Further, **3h** and **3j** also show a similar pattern in solvent-dependent fluorescence studies, indicating that acryalmide ↔ iminol isomerism occurs irrespective of the substituent present in it.

The coexistence of isomers was further demonstrated by the excitation-wavelength-dependent fluorescence emission of the selected compounds **3a**, **3m**, and **3n** in chloroform solvent, shown in Figure 9. All the compounds show two/three emission peaks at higher excitation wavelengths, i.e., at 270 nm. The increase in the excitation wavelength leads to the diminishment of the longer wavelength peak, and it completely disappeared when the sample was excited beyond 320 nm. This feature again ascertains that 2-CAA derivatives exist as acrylamide and iminol isomers and that the isomerism is facilitated by the intramolecular hydrogen bonding between the carbonyl and amide moieties.

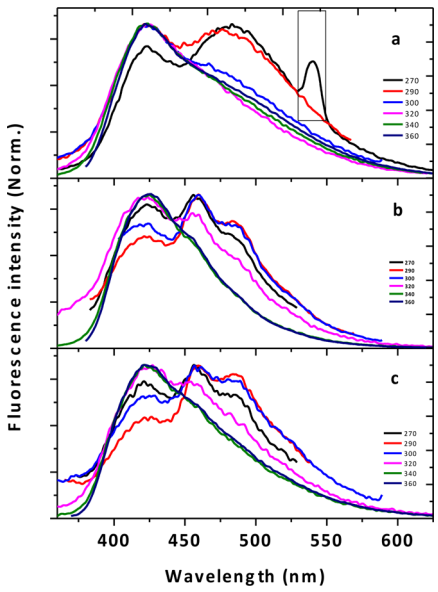

Figure 9. Excitation-wavelength-dependent fluorescence spectra of the compounds (a) **3a**, (b) **3m**, and (c) **3n** in chloroform. The peak within the rectangle in panel a is due to second-order scattering.

CONCLUSIONS

We are the first to report the synthesis of substituted 2-cyano-3-phenylacrylamide fluorophore derivatives showing fluorescence due to the presence of intermolecular hydrogen bonding between the carbonyl oxygen and amide hydrogen. The single-crystal X-ray structures and ^{1}H NMR studies show the presence of intermolecular hydrogen bonding between the carbonyl group and amide protons. The spectral properties were found to be strongly influenced by the electron-donating/withdrawing nature of the substituents and their substitution position. The phenyl group bearing an electron-donating substituent induces the intramolecular charge transfer character, which has been witnessed by the enhanced intensity of charge transfer absorption. Interestingly, the fluorescence and NMR studies suggest the presence of two isomeric forms, i.e., acrylamide and iminol, having two different emission energies. We have shown on the basis of the fluorescence studies that the equilibrium between the acrylamide and iminol can be tuned by the surrounding environment, the substituent, and its position, which would be an ideal behavior for a molecule to be used as a fluorescent probe for biological environments. We believe that our preliminary studies revealed the interesting photophysical properties of 2-cyano-3-phenylacrylamide derivatives, which have potential applications as a new class of dyes and fluorescent probes.

EXPERIMENTAL SECTION

Materials and Methods. FT-IR spectra were recorded in the range of 4000−400 cm^{-1}. ^{1}H NMR and ^{13}C NMR spectra were recorded in $CDCl_3$ and DMSO-d_6 solvents. Chemical shifts are given in parts per million (δ-scale), and the coupling constants are given in hertz. For HRMS, the ionization method was electron impact ionization (EI) and the analyzer type was magnetic field deflection double focusing (electrostatic field and magnetic field, high resolution). The steady-state fluorescence measurements were determined using a fluorescence spectrophotometer. Fluorescence lifetimes were measured by the time-correlated single-photon-counting method (IBH). The molecules were excited at 375 nm for <200 ps using Nano LED light, and the decay profiles are monitored at the respective emission maximum wavelengths. Thin layer chromatography was performed on precoated silica gel on alumina plates.

Single crystals of **3j** were grown from methanol. The structure was solved by applying the direct phase-determination technique using SHELXS-97 and refined by full-matrix least-squares on F^2 using SHLEXL-97.[17−19] Hydrogens were stereochemically fixed and refined with the riding options. The distances with the hydrogen atoms are aromatic/sp^2 C−H = 0.93 Å, amide N−H = 0.86 Å, and Uiso = 1.2Ueq(parent). Essential crystal data are listed in Table S2 (SI). Crystallographic data have been deposited at the Cambridge Crystallographic Data Center with entry number CCDC 1018088.

DOI: 10.1021/acs.joc.5b02226
J. Org. Chem. 2015, 80, 12351−12358

General Procedure for the Synthesis of Phenylacrylamide (3a−3n). A dry 100 mL Erlenmeyer flask was charged with cyanoacetamide (1.0 mmol), aromatic aldehydes (1.0 mmol), sodium hydroxide (1 mol %), and methanol (15 mL). The reaction mixture was stirred at 40 °C for 1−2 h. The reaction was monitored by TLC and after the completion of reaction, the reaction mixture was neutralized by adding a few drops of 0.1 N HCl. Thus, the reaction mixture was extracted with DCM (3 × 20 mL) and the crude reaction mixture was recrystallized using a mixture of ethanol:THF (1:1).

*2-Cyano-3-phenylacrylamide (**3a**).* Colorless crystal; mp 143−144 °C; R_f 0.73 (50% ethyl acetate:hexane); FTIR (KBr) ν 3452, 3061, 2900, 2309, 1697 cm^{-1}; ^1H NMR (400 MHz, $CDCl_3$) 5.50 (s, 1H), 6.15 (s, 1H), 6.82−6.84 (d, 2H), 6.89 (s, 1H), 7.18−7.12 (d, 2H), 7.36−7.39 (t, 1H) ppm; ^{13}C NMR (100 MHz, $CDCl_3$) 104.3, 119.5, 121.1, 121.1, 124.3, 127.9, 128.0, 165.9 ppm; HRMS calcd for $C_{10}H_8N_2O$ ($[M]^+$) 172.0637, found 172.0639.

*2-Cyano-3-(4-methoxyphenyl)acrylamide (**3b**).* Light yellow powder; mp 253−255 °C; R_f 0.62 (50% ethyl acetate:hexane); FTIR (KBr) ν 3476, 3095, 2961, 2364, 1727 cm^{-1}; ^1H NMR (400 MHz, $CDCl_3$) 3.86 (s, 3H), 5.76 (s, 1H), 6.31 (s, 1H), 6.81−6.90 (m, 2H), 7.14−7.18 (m, 2H), 7.15 (s, 1H) ppm; ^{13}C NMR (100 MHz, $CDCl_3$) 42.5, 111.0, 114.4, 120.1, 123.3, 124.7, 129.0, 129.8, 136.1, 169.7 ppm; HRMS calcd for $C_{11}H_{10}N_2O_2$ ($[M]^+$) 202.0742, found 202.0740.

*2-Cyano-3-(2-methoxyphenyl)acrylamide (**3c**).* Yellow powder; mp 261−263 °C; R_f 0.47 (50% ethyl acetate:hexane); FTIR (KBr) ν 3462, 3084, 2882, 2379, 1703 cm^{-1}; ^1H NMR (400 MHz, $CDCl_3$) 3.88 (s, 3H), 5.98 (s, 1H), 6.42 (s, 1H), 6.83−6.92 (m, 2H), 7.15−7.20 (t, 1H), 7.25 (s, 1H), 7.51−7.53 (d, 1H) ppm; ^{13}C NMR (100 MHz, $CDCl_3$) 49.9, 114.5, 125.8, 127.8, 128.5, 130.9, 134.6, 136.2, 169.6 ppm; HRMS calcd for $C_{11}H_{10}N_2O_2$ ($[M]^+$) 202.0742, found 202.0743.

*2-Cyano-3-(p-tolyl)acrylamide (**3d**).* Light white powder; mp 205−206 °C; R_f 0.53 (50% ethyl acetate:hexane); FTIR (KBr) ν 3447, 3003, 2946, 2373, 1661 cm^{-1}; ^1H NMR (400 MHz, $CDCl_3$) 2.42 (s, 3H), 5.72 (s, 1H), 6.15 (s, 1H), 6.76 (s, 1H), 7.34−7.36 (d, 2H), 7.42−7.44 (d, 2H) ppm; ^{13}C NMR (100 MHz, $CDCl_3$) 27.7, 122.2, 128.9, 129.0, 131.5, 132.2, 133.7, 134.5, 134.6, 167.8 ppm; HRMS calcd for $C_{11}H_{10}N_2O$ ($[M]^+$) 186.0793, found 186.0796.

*2-Cyano-3-(m-tolyl)acrylamide (**3e**).* Creamy powder; mp 254−256 °C; R_f 0.69 (50% ethyl acetate:hexane); FTIR (KBr) ν 3482, 3019, 2971, 2356, 1636 cm^{-1}; ^1H NMR (400 MHz, $CDCl_3$) 2.24 (s, 3H), 6.01 (s, 1H), 6.42 (s, 1H), 7.00 (s, 1H), 7.03−7.08 (t, 1H), 7.13−7.17 (t, 1H), 7.27−7.34 (q, 1H), 7.43−7.46 (d, 1H) ppm; ^{13}C NMR (100 MHz, $CDCl_3$) 26.3, 114.6, 122.4, 128.8, 129.0, 134.3, 135.0, 135.6, 167.8 ppm; HRMS calcd for $C_{11}H_{10}N_2O$ ($[M]^+$) 186.0793, found 186.0792.

*2-Cyano-3-(o-tolyl)acrylamide (**3f**).* White powder; mp 225−227 °C; R_f 0.37 (50% ethyl acetate:hexane); FTIR (KBr) ν 3483, 3094, 2953, 2328, 1643 cm^{-1}; ^1H NMR (400 MHz, $CDCl_3$) 2.21 (s, 3H), 6.08 (s, 1H), 6.45 (s, 1H), 6.91−6.95 (t, 1H), 7.09 (s, 1H), 7.24−7.28 (t, 1H), 7.44−7.46 (d, 1H), 7.58−7.61 (d, 1H) ppm; ^{13}C NMR (100 MHz, $CDCl_3$) 21.0, 114.5, 122.9, 129.3, 133.4, 135.5, 166.9 ppm; HRMS calcd for $C_{11}H_{10}N_2O$ ($[M]^+$) 186.0793, found 186.0792.

*2-Cyano-3-(4-fluorophenyl)acrylamide (**3g**).* Light yellowish powder; mp 211−212 °C; R_f 0.82 (50% ethyl acetate:hexane); FTIR (KBr) ν 3423, 3121, 2983, 2375, 1684 cm^{-1}; ^1H NMR (400 MHz, $CDCl_3$) 6.73 (s, 1H), 6.82−6.85 (d, 1H), 7.11 (s, 1H), 7.32 (s, 1H), 7.31−7.34 (d, 1H), 7.39−7.42 (d, 2H) ppm; ^{13}C NMR (100 MHz, $CDCl_3$) 112.0, 114.3, 120.0, 123.4, 125.1, 129.0, 129.6, 135.9, 168.9 ppm; HRMS calcd for $C_{10}H_7FN_2O$ ($[M]^+$) 190.0542, found 190.0544.

*2-Cyano-3-(3-fluorophenyl)acrylamide (**3h**).* Greenish powder; mp 203−205 °C; R_f 0.41 (50% ethyl acetate:hexane); FTIR (KBr) ν 3412, 3133, 2921, 2345, 1666 cm^{-1}; ^1H NMR (400 MHz, $CDCl_3$) 5.93 (s, 1H), 6.34 (s, 1H), 6.71−6.73 (d, 1H), 7.12−7.14 (d, 1H), 7.23−7.27 (t, 1H), 7.31 (s, 1H), 7.39−7.47 (m, 1H) ppm; ^{13}C NMR (100 MHz, $CDCl_3$) 114.5, 115.9, 116.1, 122.4, 123.8, 124.0, 129.4, 130.3, 136.1, 166.8 ppm; HRMS calcd for $C_{10}H_7FN_2O$ ($[M]^+$) 190.0542, found 190.0540.

*2-Cyano-3-(2-fluorophenyl)acrylamide (**3i**).* Light greenish powder; mp 227−229 °C; R_f 0.63 (50% ethyl acetate:hexane); FTIR (KBr) ν 3450, 3093, 2930, 2339, 1671 cm^{-1}; ^1H NMR (400 MHz, $CDCl_3$) 6.93−6.97 (t, 2H), 7.18 (s, 1H), 7.26−7.31 (m, 1H), 7.28 (s, 1H), 7.46 (s, 1H), 7.61−7.63 (d, 1H) ppm; ^{13}C NMR (100 MHz, $CDCl_3$) 114.5, 114.9, 122.9, 128.0, 128.6, 128.8, 128.9, 135.6, 136.7, 167.9 ppm; HRMS calcd for $C_{10}H_7FN_2O$ ($[M]^+$) 190.0542, found 190.0543.

*2-Cyano-3-(4-cholorophenyl)acrylamide (**3j**).* Light yellow crystal; mp 238−240 °C; R_f 0.52 (50% ethyl acetate:hexane); FTIR (KBr) ν 3473, 3094, 2952, 2373, 1642 cm^{-1}; ^1H NMR (400 MHz, DMSO) 7.63−7.65 (d, 2H), 7.83 (s, 1H), 7.94−7.96 (d, 2H), 7.96 (s, 1H), 8.18 (s, 1H) ppm; ^{13}C NMR (100 MHz, DMSO) 110.5, 121.3, 124.6, 127.6, 127.7, 164.6 ppm; HRMS calcd for $C_{10}H_7ClN_2O$ ($[M]^+$) 206.0247, found 206.0245.

*2-Cyano-3-(2-cholorophenyl)acrylamide (**3k**).* White powder; mp 208−209 °C; R_f 0.26 (50% ethyl acetate:hexane); FTIR (KBr) ν 3485, 3103, 2894, 2356, 1742 cm^{-1}; ^1H NMR (400 MHz, DMSO) 7.32 (s, 1H), 7.89 (s, 1H), 7.38−7.51 (d, 2H), 7.89−7.92 (d, 2H), 8.20 (s, 1H) ppm; ^{13}C NMR (100 MHz, DMSO) 114.6, 125.2, 129.4, 129.5, 136.9, 167.4 ppm; HRMS calcd for $C_{10}H_7ClN_2O$ ($[M]^+$) 206.0247, found 206.0246.

*2-Cyano-3-(4-bromophenyl)acrylamide (**3l**).* Light brown powder; mp 257−258 °C; R_f 0.64 (50% ethyl acetate:hexane); FTIR (KBr) ν 3459, 3041, 2978, 2329, 1681 cm^{-1}; ^1H NMR (400 MHz, $CDCl_3$) 5.68 (s, 1H), 6.23 (s, 1H), 6.83 (s, 1H), 7.33−7.35 (d, 2H), 7.40−7.42 (d, 2H) ppm; ^{13}C NMR (100 MHz, $CDCl_3$) 122.0, 127.5, 128.7, 128.8, 131.9, 132.1, 133.7, 135.9, 168.2 ppm; HRMS calcd for $C_{10}H_7BrN_2O$ ($[M]^+$) 249.9742, found 249.9743.

*2-Cyano-3-(4-cyanophenyl)acrylamide (**3m**).* Light yellow powder; mp 281−282 °C; R_f 0.42 (50% ethyl acetate:hexane); FTIR (KBr) ν 3474, 3051, 2892, 2346, 1701 cm^{-1}; ^1H NMR (400 MHz, $CDCl_3$) 5.62 (s, 1H), 5.89 (s, 1H), 6.73 (s, 1H), 6.82−6.84 (d, 2H), 6.94−6.96 (d, 2H) ppm; ^{13}C NMR (100 MHz, $CDCl_3$) 123.1, 125.3, 129.6, 130.5, 131.5, 135.7, 137.6, 169.9 ppm; HRMS calcd for $C_{11}H_7N_3O$ ($[M]^+$) 197.0589, found 197.0591.

*2-Cyano-3-(naphthalen-1-yl)acrylamide (**3n**).* Colorless crystal; mp 245−246 °C; R_f 0.88 (50% ethyl acetate:hexane); FTIR (KBr) ν 3471, 3068, 2953, 2329, 1681 cm^{-1}; ^1H NMR (400 MHz, $CDCl_3$) 6.51 (s, 1H), 6.85 (s, 1H), 6.84−6.86 (d, 1H), 7.44−7.54 (m, 4H), 7.82−7.84 (d, 1H), 7.89−7.90 (d, 1H), 8.22−8.24 (d, 1H) ppm; ^{13}C NMR (100 MHz, $CDCl_3$) 114.5, 122.6, 123.7, 124.8, 125.9, 126.1, 127.1, 128.6, 129.4, 131.0, 132.3, 133.8, 136.6, 167.8 ppm; HRMS calcd for $C_{14}H_{10}N_2O$ ($[M]^+$) 222.0793, found 222.0792.

■ ASSOCIATED CONTENT

Supporting Information

The Supporting Information is available free of charge on the ACS Publications website at DOI: 10.1021/acs.joc.5b02226.

Table summarizing synthetic conditions, spectroscopic characterization of all compounds, HOMO and LUMO of 2-CAA derivatives, crystal data for **3j**, and Cartesian coordinates for **3a−i,k−m** (PDF)

Crystallographic data in CIF format for **3j** (CIF)

■ AUTHOR INFORMATION

Corresponding Authors

*K.I.S. E-mail: sathiya_kuna@hotmail.com.

*S.E. E-mail: moorthi@clri.res.in.

Present Address

(R.S.R.) Department of Biotechnology, DSCE, Dayanandasagar Institute, Bangalore 560 078, India.

Author Contributions

R.G. and P.T. contributed equally to this work.

Notes

The authors declare no competing financial interest.

DOI: 10.1021/acs.joc.5b02226
J. Org. Chem. 2015, 80, 12351−12358

■ ACKNOWLEDGMENTS

The work is supported by the suprainstitutional project "STRAIT" of CSIR-CLRI. P.T. acknowledges the Department of Science and Technology for the INSPIRE fellowship. The DST-FIST NMR facility at VIT University is greatly acknowledged. We also thank Prof. P. Ramamurthy and Dr. C. Selvaraju, NCUFP, University of Madras, for their help with fluorescence lifetime measurements. This work is CSIR-CLRI contribution no. 1094.

■ REFERENCES

(1) Gonçalves, M. S. T. *Chem. Rev.* **2009**, *109*, 190.
(2) Keeling-Tucker, T.; Brennan, J. D. *Chem. Mater.* **2001**, *13*, 3331.
(3) Holzhauser, C.; Wagenknecht, H.-A. *J. Org. Chem.* **2013**, *78*, 7373.
(4) Beija, M.; Afonso, C. A. M.; Martinho, J. M. G. *Chem. Soc. Rev.* **2009**, *38*, 2410.
(5) Stennett, E. M. S.; Ciuba, M. A.; Levitus, M. *Chem. Soc. Rev.* **2014**, *43*, 1057.
(6) An, B.-K.; Gierschner, J.; Park, S. Y. *Acc. Chem. Res.* **2012**, *45*, 544.
(7) Li, Y.; Li, F.; Zhang, H.; Xie, Z.; Xie, W.; Xu, H.; et al. *Chem. Commun.* **2007**, *3*, 231.
(8) Javed, I.; Zhou, T.; Muhammad, F.; Guo, J.; Zhang, H.; Wang, Y. *Langmuir* **2012**, *28*, 1439.
(9) Zhang, Y.; Liang, C.; Shang, H.; Ma, Y.; Jiang, S. *J. Mater. Chem. C* **2013**, *1*, 4472.
(10) Song, Q.; Chen, K.; Sun, J.; Wang, Y.; Ouyang, M.; Zhang, C. *Tetrahedron Lett.* **2014**, *55*, 3200.
(11) Pietrzak, M.; Bajorek, A. *Dyes Pigm.* **2013**, *96*, 63.
(12) Bosch, P.; Fernández-Arizpe, A.; Mateo, J. L.; Corrales, T.; Peinado, C. *J. Photochem. Photobiol., A* **2004**, *167*, 229.
(13) Bosch, P.; Fernández-Arizpe, A.; Mateo, J. L.; Catalina, F.; Peinado, C. *J. Photochem. Photobiol., A* **2002**, *153*, 135.
(14) Bosch, P.; Fernández-Arizpe, A.; Mateo, J. L.; Lozano, A. E.; Noheda, P. *J. Photochem. Photobiol., A* **2000**, *133*, 51.
(15) Valdenaire, A.; Pothier, J.; Renneberg, D.; Riederer, M. A.; Peter, O.; Leroy, X.; et al. *Bioorg. Med. Chem. Lett.* **2013**, *23*, 944.
(16) Song, Q.; Chen, K.; Sun, J.; Wang, Y.; Ouyang, M.; Zhang, C. *Tetrahedron Lett.* **2014**, *55*, 3200.
(17) Suresh, J. S.; Sandhu. *Green Chem. Lett. Rev.* **2009**, *2*, 189.
(18) Ramachandran, G.; Raman, A.; Easwaramoorthi, S.; Rathore, R. S.; Sathiyanarayanan, K. *RSC Adv.* **2014**, *4*, 29276.
(19) Frisch, M. J.; Trucks, G. W.; Schlegel, H. B.; Scuseria, G. E.; Robb, M. A.; Cheeseman, J. R.; et al. *Gaussian 03*, Rev. E.01; Gaussian, Inc.: Wallingford, CT, 2004.
(20) Hansch, C.; Leo, A.; Taft, R. W. *Chem. Rev.* **1991**, *91*, 165.
(21) Hammett, L. P. *J. Am. Chem. Soc.* **1937**, *59*, 96.
(22) Programs used: Bruker (2004) APEXII (Version 108), SAINT-Plus (Version 723A), and SADABS (Version 2004/1) from Bruker AXS Inc. and USAOR from Oxford Diffraction.
(23) Farrugia, L. *J. Appl. Crystallogr.* **1997**, *30*, 565.
(24) Sheldrick, G. *Acta Crystallogr., Sect. A: Found. Crystallogr.* **2008**, *64*, 112.

DOI: 10.1021/acs.joc.5b02226
J. Org. Chem. 2015, 80, 12351−12358